Journal of the European Ceramic Society **12** (1993) 315–321

Micromachining of Ceramics with Excimer Laser Radiation

M. Goller*

Institut für Werkstoffwissenschaften 3, Universität Erlangen-Nürnberg, Martensstrasse 5, W-8520 Erlangen, Germany

N. Lutz & M. Geiger

Lehrstuhl für Fertigungstechnologie, Universität Erlangen-Nürnberg, Egerlandstrasse 11, W-8520 Erlangen, Germany

(Received 8 December 1992; accepted 29 March 1993)

Abstract

A XeCl excimer laser ($\lambda = 308\,nm$) was used for investigating the possibilities of micromachining ceramic materials. The influence of the optical setup and laser parameters on the processing quality has been determined, as well as the behaviour of various ceramic materials during the machining process. The machining results and the structure quality are discussed concerning the shape of the holes, break-outs in the structure and the homogeneity of the hole depth and size. Optical microscopy and SEM investigations served as the main tools for the characterization. Strategies for large area micromachining were investigated to achieve a very large number of high quality microstructures.

Ein XeCl-Excimerlaser ($\lambda = 308\,nm$) wurde zur Mikrostrukturierung keramischer Werkstoffe eingesetzt. Schwerpunkte der Untersuchungen waren der Einfluß des optischen Aufbaus und der verschiedenen Laserparameter auf die Bearbeitungsqualität und die durch den Bearbeitungsprozeß verursachten Werkstoffveränderungen verschiedener keramischer Materialien. Die Form der durch Abtragung erzeugten Strukturen, Ausbruchserscheinungen sowie die Homogenität der Lochtiefen und -größen dienen zur Beschreibung der Bearbeitungsergebnisse. Lichtmikroskopie und REM-Untersuchungen wurden für die Probencharakterisierung herangezogen. Strategien zur großflächigen Bearbeitung wurden mit der Zielsetzung entwickelt, eine sehr große Anzahl von Mikrostrukturen mit hoher Bearbeitungsqualität zu erzeugen.

On a utilisé un laser excimer XeCl ($\lambda = 308\,nm$) pour étudier les possibilités de microstructurer les matériaux céramiques. On a déterminé l'influence de la construction optique et des paramètres du laser sur la qualité du procédé, ainsi que le comportement des différentes céramiques durant le procédé de fabrication. Les résultats de fabrication et la qualité de la structure sont discutés en rapport avec la forme des trous, les éruptions dans la structure et l'homogénéité de la profondeur et de la taille des trous. Les observations par microscopie optique et MEB sont les outils principaux utilisés pour la caractérisation. On a étudié des stratégies pour travailler de grandes surfaces dans le but d'obtenir un trés grand nombre de microstructure de trés bonne qualité.

* Present address: Alfred University, New York State College of Ceramics, Alfred, NY 14802, USA.

1 Introduction

Applications in the medical field brought up the necessity for a high-resolution radiation detector based on a ceramic radiation-sensitive material, e.g. an alkaline earth halogenide. The mechanism of the readout process in the detector required a partition of the surface in very small single cells to obtain the desired high spatial resolution.

Two strategies were investigated in the experiments to achieve this objective:

—A massive sample of the sensitive material is carved into small trenches with a depth of 300 μm and width of 10–20 μm. The resulting cells will be $50 \times 50\,\mu m^2$ in cross-section. This strategy is called positive structuring.

—Blind holes with a cross-section of $50 \times 50\,\mu m^2$ and a depth of 300 μm have to be machined out

Journal of the European Ceramic Society 0955-2219/93/$6.00

of a ceramic. The remaining partition walls between the holes should not exceed 20 μm in thickness. This method is called negative structuring. The machined ceramic will serve as a substrate for the radiation-sensitive material.

Due to the small dimensions and the unusually high aspect ratio of the requested structures, laser machining was chosen as a good possibility to handle the problem. The low thermal effects in most materials induced by the excimer laser radiation compared to CO_2 laser or Nd:YAG laser radiation[1] were promising for the experiments.

2 Experimental Setup

The XeCl excimer laser ($\lambda = 308$ nm) is characterized by a high pulse energy of 2 J, a pulse duration of 50 ns, a maximum pulse frequency of 20 Hz and a large homogeneous beam cross-section of $45 \times 55\,mm^2$. For large area machining, a high-resolution x–y-linear stage as a target positioning system is adapted.[2]

The setup uses a mask projection technique which offers advantages compared to contact mask techniques. The main advantage of the scale-down principle of the projection is that it allows high precision structures in the μm region which are impossible to obtain with contact masks.

For the negative structuring method etched stainless steel masks (thickness 0·2 mm) in various geometries were used. The positive structuring was performed with fused silica substrates plated with a structured chromium coating.

The selection of substrate materials to be machined covered the whole spectrum in the ceramic field: oxides, nonoxides, ceramics with high and low thermal conductivity and thermal expansion coefficient. For the desired application, the adaption of the ceramic substrate to the radiation-sensitive material also set restrictions.

The following ceramics were investigated:

Oxides:	Al_2O_3 R 708 and R 710, Al_2TiO_5, ferrite, ZrO_2 (Mg-stabilized).
Nonoxides:	SiC, SiC ($+TiB_2$), SiSiC, Si_3N_4 (various modifications), graphite.

The optical setup and the laser parameters were varied to get a deeper understanding of the machining process of these materials.

The investigations concerning the optical setup should give information about the influence of adjustment of the lenses and the tolerances that can be allowed, while still receiving a suitable micromachining result. That covers homogeneous hole depths across the whole area, optimized structure quality and the obtainable minimum structure size. The imaging lens was systematically maladjusted perpendicular to the optical axis to deliver that information. Another point of interest was the influence of the mask geometry on ablation parameters like ablation rate and the inclination angle of the structure walls. For these experiments a rebuilt single lens reflex camera lens aperture served as a variable mask. For very small structures below 100 μm in diameter, etched masks were used. The investigations covering the optical setup and mask geometry were carried out using Al_2O_3 R 708 as a target material.

Laser parameters to be varied are pulse frequency, pulse number and energy density at the target. The energy density was changed through variations of the optical setup and, as a result, the imaging scale.

Optical microscopy and SEM studies provided information concerning the quality of the structures. Profilometry was used to analyse the depth and geometry of the samples. X-Ray fluorescence analysis measurements were carried out to investigate possible changes in the surface composition of the material. Measurements of the thermal diffusivity were made to find a correlation between material properties and ablation parameters. The plasma plume was photographed with a standard single lens reflex camera. The change in shape and colour for various depths was documented.

3 Results

3.1 Optical setup and mask geometry

The adjustment of the optical setup plays an important role for high quality structuring. Maladjustment of the imaging lens perpendicular to the optical axis leads to variations in hole depth. The bottom of a $1 \times 1\,mm^2$ square hole is then tilted depending on the direction and magnitude of maladjustment. Satisfactory machining results can be obtained when the adjustment perpendicular to the optical axis is performed within $\pm 0{\cdot}5$ mm. Inhomogeneous hole depths and distorted images of the mask are observed for larger maladjustments.

Maladjustment parallel to the optical axis obviously leads to a defocused image and in consequence to nonuniform processing.[3] According to the desired minimum structure size, focusing with an accuracy of 100 μm is necessary. All experiments were carried out with the imaging plane set on the target surface. The effect of the interacting surface moving out of the ideal adjustment during the machining process due to ablation was not addressed in this work.

The mask geometry affects important ablation parameters such as the ablation rate.[4,5] Smaller sizes of the machined area result in an increased ablation rate, as shown in Fig. 1 for Al_2O_3 R 708. Figure 2

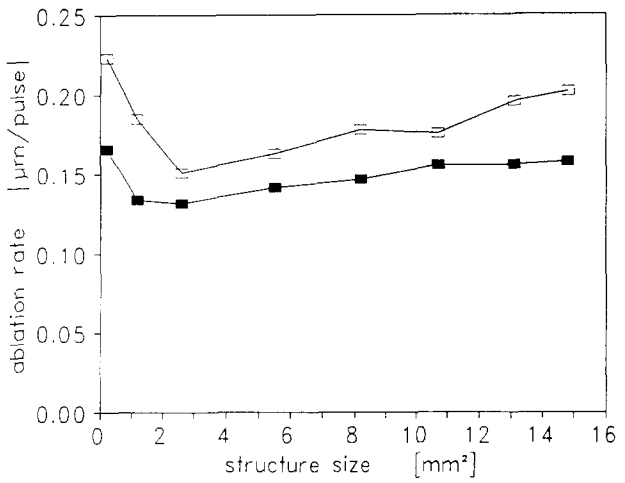

Fig. 1. Increase of ablation rates with decreasing structure size, Al_2O_3 R708. $H_E = 10\,J/cm^2$. □, $f_p = 1$ Hz; ■, $f_p = 20$ Hz.

shows the influence of the energy density on the ablation rate for SiC and Si_3N_4. A similar effect was observed for all materials, but at a structure size of $25 \times 75\,\mu m^2$, the maximum ablation rate seems to be reached. Materials with an extraordinary high ablation rate, e.g. graphite, showed a decrease of the ablation rate for structure sizes smaller than $25 \times 75\,\mu m^2$. The plasma expansion behaviour is one main reason for the increase of the ablation rate. The plasma plume expands in a three-dimensional way for large structures (e.g. $1 \times 1\,mm^2$). On the other hand, an oriented jet-like plasma expansion can be observed for small structures. This more effective orientated plasma expansion, in combination with an increased mechanical impulse, may lead to higher ablation rates. For very small hole sizes and large depths, the ablated material is hindered from leaving the hole and it resolidifies on the inner wall of the hole. The decrease of the ablation rate for structures in the 10 μm region due to this effect was reported in Ref. 5. The experiments on Al_2O_3 with $10 \times 10\,\mu m^2$

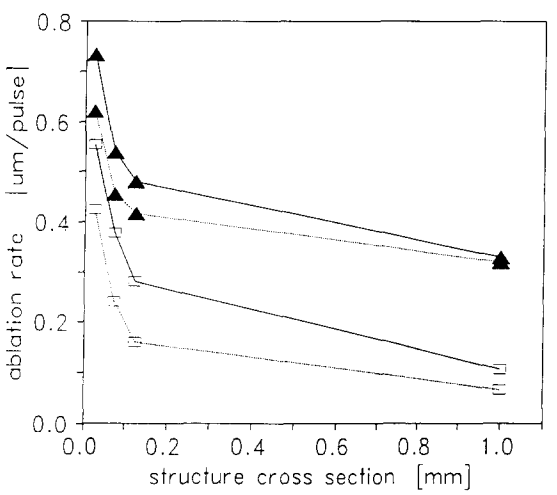

Fig. 2. Increase of ablation rates with decreasing structure cross-section dependent on energy density, $f_p = 10$ Hz. ▲, Si_3N_4, $H_E = 20\,J/cm^2$; –▲–, Si_3N_4, $H_E = 10\,J/cm^2$; –⊟–, SiC, $H_E = 20\,J/cm^2$; –⊟–, SiC, $H_E = 10\,J/cm^2$.

structures confirmed these results. Due to the small depths obtained the optical setup could be used only for precise marking of ceramics.

Thermal effects were not measured, but it is reported that the thermal conduction and, therefore, the temperature in the irradiated area depends on the size of the structure. The heating of the target as a function of beam spot size and pulse frequency was calculated in Ref. 6.

3.2 Laser parameters

The pulse frequency was varied between 1 Hz and 20 Hz. A slight decrease of the ablation rate at higher frequencies was measured for alumina, as shown for $f_p = 20$ Hz in Fig. 1. This is explained by the change in viscosity of the glass phase in the material resulting from higher temperatures. A good compromise for processing speed and the quality of the structure and the sample surface was found to be $f_p = 10$ Hz.

The most common way to affect the ablation parameters is to vary the energy density at the target. In the investigated range, higher energy densities offer higher ablation rates (see Fig. 2). The quality of the microstructures limited the energy density to a maximum of $10\,J/cm^2$.

Higher energy densities, e.g. $25\,J/cm^2$, are accompanied by disturbing thermal effects like increased melt phases in the irradiated area, increased deposits in the surroundings of the irradiated area and an increase of break-outs in the structure. This is very critical when small elements are machined (Fig. 3). The ablation rates of the ceramic materials listed in Fig. 4 are in good agreement with some values from the literature.[4]

3.3 Material aspects

The ceramic materials showed characteristic reactions under XeCl excimer laser irradiation, but there are some common aspects. Unless noted, all reported effects refer to the negative structuring technique, but for positive structuring similar phenomena are observed.

Oxides are characterized by melted phases covering the structure walls and, using high energy densities, also covering the surroundings of the machined area. The oxidic materials also show typical colours which are a result of solid-state electronic defects. The surface of Al_2O_3 is covered with a grey shade due to the formation of colour centres, which can be recombined by heat treatment. In the microstructuring experiments, the heating through the conducted heat was efficient enough to decolourize the material. Al_2TiO_5 shows an intense blue to black colour that is also spread beyond the irradiated area. TiO_2 partially reduced to TiO_{2-n} with $0 < n < 0{\cdot}5$ is assumed to be responsible for the

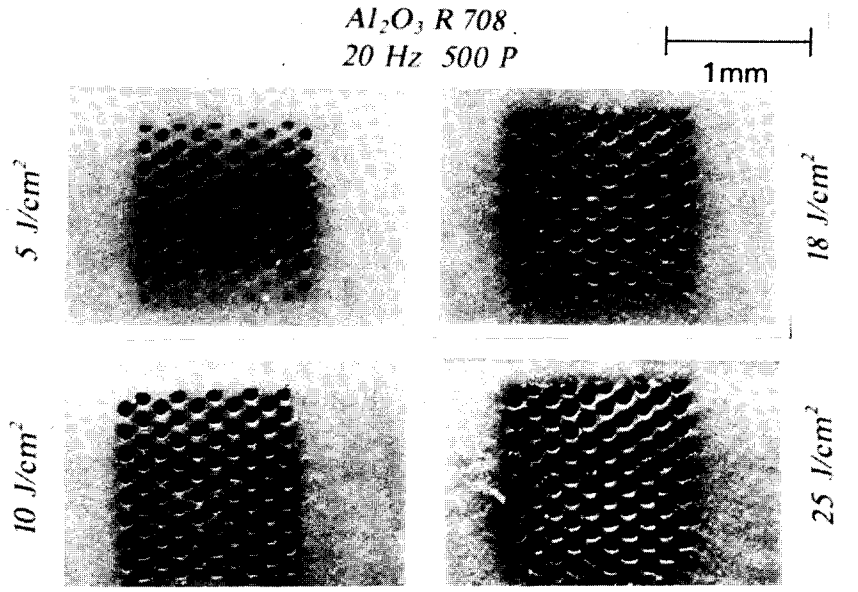

Fig. 3. Influence of energy density on processing quality, Al_2O_3 R708; ablation threshold at $H_E \sim 5$ J/cm^2, hole diameter 100 μm.

effect.[7] Only heavy thermal treatment can remove the colour.[8]

Zirconia also shows a black coloured area due to a reduction process. The colouring is sharply limited to the area irradiated by the excimer laser, while the surroundings are not influenced. ZrO_2 shows a unique effect at energy densities below 10 J/cm^2 and large structures (e.g. 1 × 1 mm^2). The melted phase is not removed completely and small resolidified particles can still be found even using high pulse numbers. The mechanism of that effect is under further investigation. Zirconia is also unique in its surface structure after irradiation. Figure 5 shows the SEM micrograph of a cross-section through the edge of a ZrO_2 wall. A similar structure was found at the bottom of the structure. A transparent layer of melted and resolidified ZrO_2 covers a coloured layer on the treated area. Under this layer the unaffected bulk ZrO_2 is observed.

Nonoxides normally show no melted phases of substrate material. Characteristic melted phases of decomposed material are observed for these ceramics. SiC and SiSiC exhibit a silicon-coated irradiated area. The silicon builds walls that exceed the surface level. Si_3N_4 and graphite show no melted phases at all. The products of decomposition of SiC and Si_3N_4 can be found as deposits around the machined area. Their amounts and shapes differ for various manufacturers. SiO_2 is the main component in these deposits. On SiC, the SiO_2 appears as a powder-like phase which can be removed easily, on Si_3N_4 the deposits form a solid layer.

Typical cross-sections of SiC/SiSiC and Si_3N_4 are shown in Fig. 6. The steep wall for SiSiC is

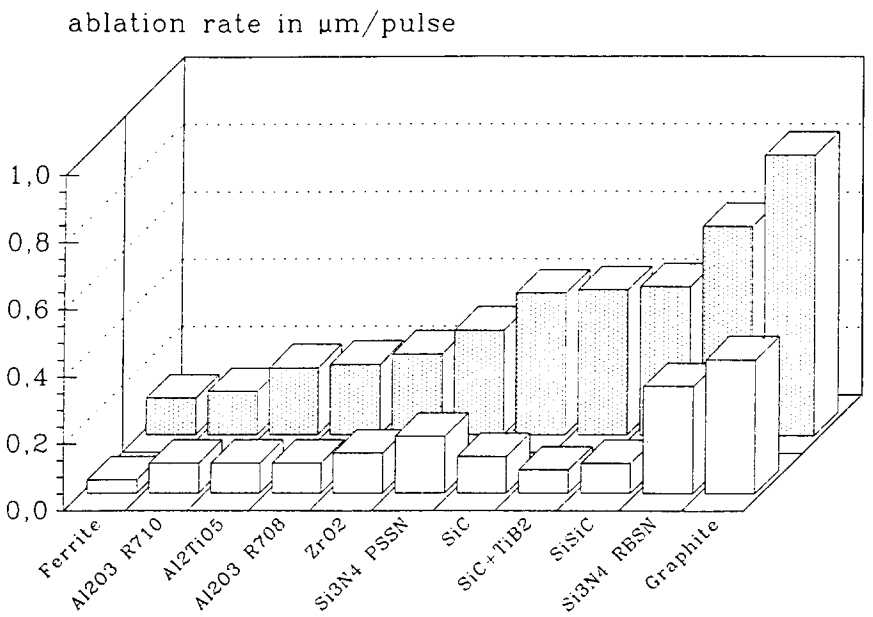

Fig. 4. Ablation rates of the investigated ceramic materials. The influence of the structure size is demonstrated. □, 1 × 1 mm^2; ▨, 25 × 75 μm^2.

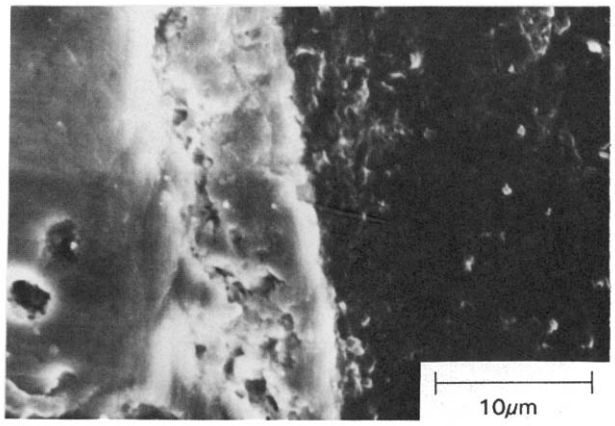

Fig. 5. Cross-section of the edge of a wall in ZrO_2, $H_F = 10\,J/cm^2$, $N = 500$; resolidified layer on bulk material (right side).

remarkable. Large inclination angles of the walls are also typical for structures in SiC. A resolidified silicon phase already mentioned is observed, creating a metallic layer on the bulk material. Additional phases in SiC, e.g. TiB_2 in this case. do not have a significant influence on the ablation behaviour.

Si_3N_4 is also characterized by very steep walls. However, here, in the upper part of the structure, a decrease of the inclination angle is obvious. A possible explanation is a change in the behaviour of the expanding plasma at various depths. As already mentioned, within small and deep structures a jet-like plasma that is mainly orientated perpendicular to the interacting surface is observed. Large inclination angles are a result of these conditions. Near the surface the plasma expansion is considered to be more three dimensional and causes lower inclination angles.

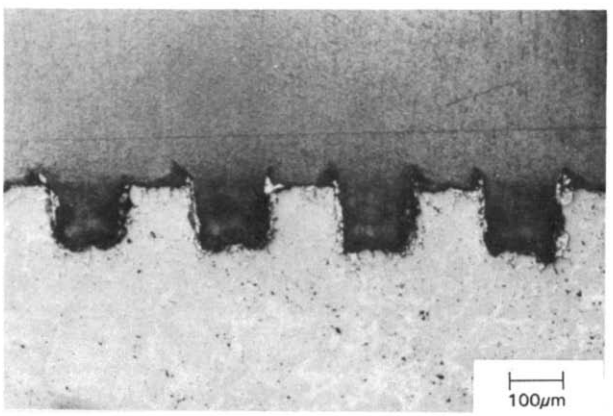

(a)

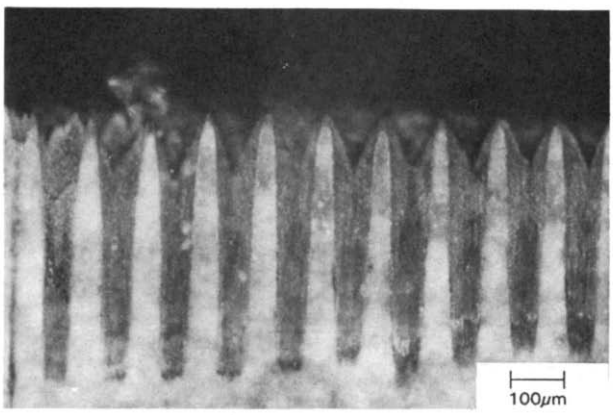

(b)

Fig. 6. (a) SiSiC, $H_F = 20\,J/cm^2$, $N = 250$, structure size $125 \times 125\,\mu m^2$, (b) Si_3N_4, $H_F = 20\,J/cm^2$, $N = 1000$, structure size $25 \times 75\,\mu m^2$.

Graphite exposed to energy densities up to $10\,J/cm^2$ reveals high quality structuring without any melted phases or large influence on the surroundings. The deposited carbon can be removed easily. In contrast with SiC/SiSiC and Si_3N_4 there is no increase of the inclination angle even in small structures. This leads to the effect that the walls come into contact for large depths. This phenomenon requires further investigation.

Generally, the wall inclination angle is assumed to be a function of the energy density and the ablation threshold of the material.[4,9] The reported increase with higher energy densities could be confirmed only for large structure sizes and low pulse numbers. Especially regarding the results on Si_3N_4, small and deep structures exhibit a different behaviour.

Examples of both structuring techniques are shown in Fig. 7. The positive structuring was done on Si_3N_4. Hexagonal structures in a honeycomb arrangement are the structure design. This special design shows a nonoptimal processing quality caused by material erosion during plasma expansion at the top of the structures. Increasing inclination angles with depth are obvious. Melted phases on top of the walls are observed for the negative structuring of Al_2O_3 R 708 as target material.

3.4 Large area machining

The possibilities of machining larger areas have been investigated to achieve a very large number of high quality microstructures. A similar multi-element structuring technique was recently reported.[10] Al_2O_3 R 708 and ZrO_2 served as target materials. New problems were expected due to the necessity of joining single elements to one large area, in this case 4×4 elements.

The first method consisted of machining one element to its final depth (1000 pulses), then moving the target and machining the next element. The accuracy of the final structure demonstrated the reproducibility of the target movement. This method revealed problems due to deposition of ablated material in already machined areas.

Better results were obtained using a 'multiscan technique'. Single elements are machined with a smaller pulse number (in this case 100 pulses). All elements of the whole structure are machined

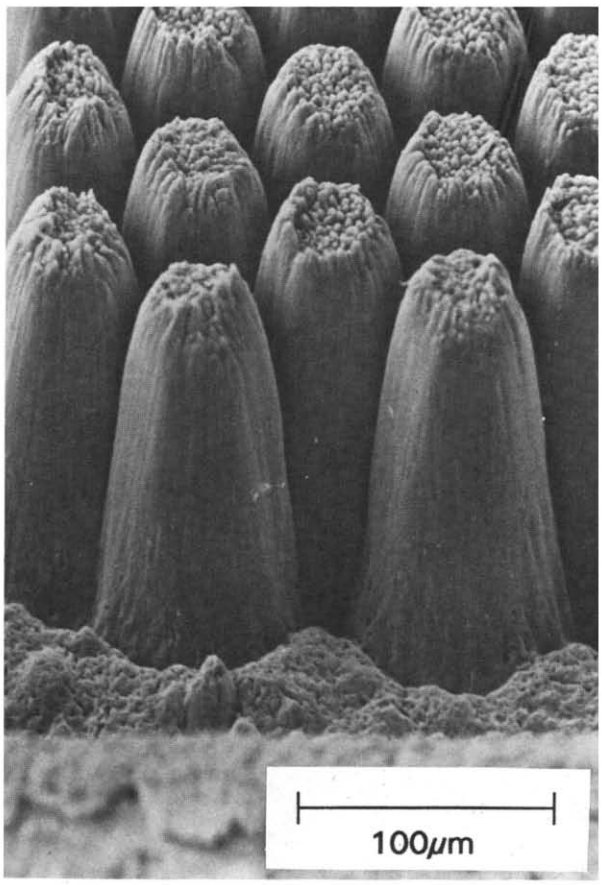

(a)

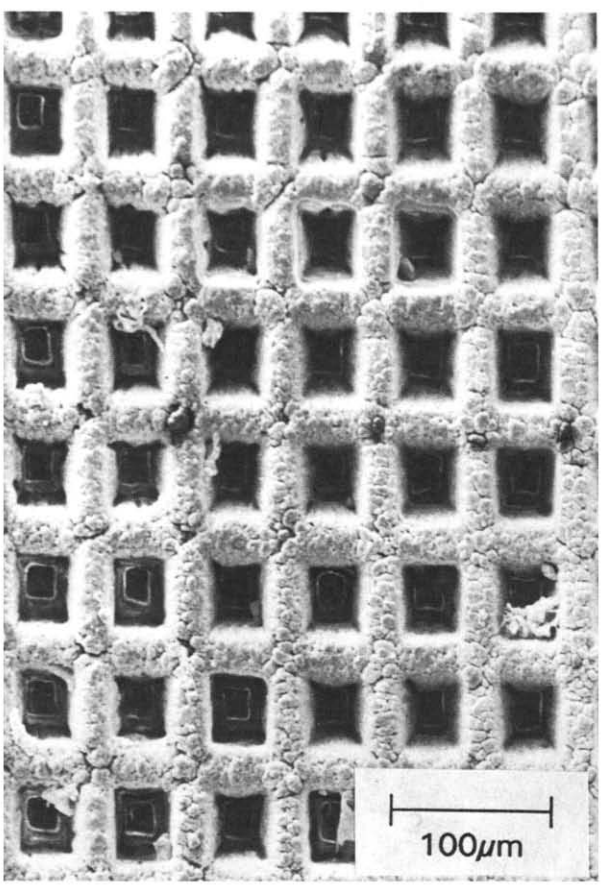

(b)

Fig. 7. (a) Positive structuring of Si_3N_4, $H_E = 12\,J/cm^2$, $N = 500$, (b) negative structuring of Al_2O_3, $H_E = 17{\cdot}5\,J/cm^2$, $N = 1000$, 'multiscan technique'.

successively and then the procedure is repeated. The accuracy of the stage was sufficient to secure a precise positioning even after 10 cycles. The last scans were made with only 50 pulses to improve the structure quality. On machining alumina, the tops of the walls are still covered with melt phases. They can be reduced when an additional excimer laser treatment with an energy density slightly higher than the ablation threshold is performed on the finished structure.

The main advantage of the 'multiscan technique' is the removal of deposits from the holes. The quality of the top of the walls is improved. The quality of contact lines between two elements could be improved when the target was moved only half the size of an element. A large area structure with a very uniform appearance was obtained by this technique.

4 Conclusions

Different strategies to obtain microstructures on large areas in ceramics by XeCl excimer laser micromachining were determined. The desired structure size of $25 \times 75\,\mu m^2$ at $300\,\mu m$ depth was reached in the experiments. Machining is accompanied with changes of very shallow layers of the material in the irradiated area. A 'multiscan technique' was developed to machine large areas. Deposits could be reduced and the appearance was improved. This technique, in combination with the determined ablation parameters should open the possibility for using the excimer laser as a microstructuring tool for various applications. Further investigations are necessary to optimize the structure quality concerning deposits and the zones between the elements. In general, larger elements have to be achieved to get a more economic machining process.

Acknowledgements

The investigations were funded by the Bundesministerium für Forschung und Technologie (Contract No. 13N5629). The authors gratefully acknowledge support from Rofin Sinar Laser, Hoechst AG, Hoechst Ceram Tec and Linde AG. Special thanks to G. Tomandl at the Institut für Werkstoffwissenschaften 3 (WW3) for scientific advice.

References

1. Poulin, D., Eisele, P. & Znotins, T., Advances in excimer laser materials processing: An update. *SPIE Proceedings*, Vol. 1023, *Excimer Lasers and Applications*, 1988, pp. 202–7.
2. Goller, M., Tomandl, G., Lutz, N. & Geiger, M., Excimer laser radiation—a promising tool for microstructuring ceramics. *Lasers in Engineering*, submitted.

3. Geiger, M., Lutz, N., Rebhan, T. & Hutfless, J., Quality control during excimer laser materials processing. In *Proc. Gas Flow and Chemical Lasers (GCL '92), Proc. SPIE*, in press.
4. Sowada, U., Lokai, P., Kahlert, H.-J. & Basting, D., Excimer laser processing of ceramics—results and physical processes. *Laser und Optoelektronik*, **21**(3) (1989) 107–15.
5. Eyett, M. & Bäuerle, D., Influence of the beam spot size on ablation rates in pulsed-laser processing. *Appl. Phys. Lett.*, **51**(24) (1987) 2054–5.
6. Miyamoto, I. & Maruo, H., Processing of ceramics by Excimer Lasers. In *Proceedings SPIE*, Vol. 1279, *Laser-Assisted Processing II*, 1990, pp. 66–76.
7. Dance, B., Novel excimer laser system marks wires on-the-fly. *Laser Magazin*, (1) (1991) 30–1.
8. Geiger, M., Lutz, N. & Rebhan, I., Influence of process and material parameters on ablation phenomena and mechanical properties of ceramics and composites for excimer laser treatment. In *Proc. ECLAT '92*, 1992, pp. 577–84.
9. Basting, D. & Sowada, U., *Excimer Laser Applications, NATO ASI Series B*, Vol. 132, *Physics of New Laser Sources*. Plenum Press, 1985, pp. 33–9.
10. Tönshoff, H. K. & Mommsen, J., Process of generating 3-D microstructures using excimer lasers. *Laser und Optoelektronik*, **24**(1) (1992) 64–7.